Acta Geodyn. Geomater., Vol. 14, No. 2 (186), 205–220, 2017
DOI: 10.13168/AGG.2017.0004
journal homepage: https://www.irsm.cas.cz/acta

ORIGINAL PAPER

EVALUATION OF THE AMBIGUITY RESOLUTION AND DATA PRODUCTS FROM DIFFERENT ANALYSIS CENTERS ON ZENITH WET DELAY USING PPP METHOD

Sorin NISTOR* **and Aurelian Stelian BUDA**

[1)]*University of Oradea, Barbu Stefanescu Delavrancea Street no. 4, Oradea, Romania*

**Corresponding author's e-mail:* sonistor@uoradea.ro

ARTICLE INFO

Article history:
Received 19 July 2016
Accepted 1 February 2017
Available online 16 February 2017

Keywords:
PPP
Zenith wet delay
Precise ephemeris and clocks
Ambiguity resolution

ABSTRACT

The evolution of the Global Navigation Satellite System (GNSS) permitted the development of GNSS meteorology. The present article is studying the impact of ambiguity resolution and final data products on Zenith Wet Delay (ZWD). The data products were provided by different Analysis Centers (AC's) like, European Space Agency (ESA), International GNSS Service (IGS) and Jet Propulsion Laboratory (JPL). The estimation of the ZWD was made by using the Precise Point Positioning (PPP) technique. For the study we used eight European IGS stations. In the first part of the analysis the effect of data products from different AC's was analyzed. By differentiating the results of the ZWD in which we have used the data products from IGS and ESA, the ZWD presented a variation of 2 cm with a maximum of 3.2 cm on GANP station. The largest difference on the ZWD standard deviation by using precise ephemeris and clock data from different AC's were 0.2 mm, when the IGS and JPL data product were used. Using the data products from IGS and ESA, in terms of estimated ZWD standard deviation, they were in agreement of 0.1 mm. The effect of the ambiguity resolution, by using the data products from the same AC's revealed a relatively different behavior of the ZWD, only the JPL data products between the solved and unresolved ambiguities presented a similar behavior. The common part in all of the processing strategy, for the ambiguity resolution, was the use of phase biases provided by JPL.

INTRODUCTION

The Precise Point Positioning (PPP) determination was pioneered by (Zumberge et al., 1997) where large GPS (Global Positioning System) data, needed to be processed. By using final orbits and clock data products from International GNSS Service (IGS) (Heroux et al., 2001) demonstrated that this technique can achieve centimeter level accuracy but also is able to achieve homogeneous position accuracy (Dow et al., 2009; Dixon, 2006). By using the State Space Representation (SSR) information (e.g. IGS products) which describes each individual GNSS error, including atmospheric effects and by using the PPP method, the observations from a single dual frequency GNSS receiver can be used for precise positioning application. One of the main factors, that limit the accuracy of the Global Navigation Satellite System (GNSS) is represented by tropospheric refraction, among other sources of errors, like the ionospheric refraction, multipath and signal obstruction. The obtained coordinates on a long period of time, should be subject to time series analysis to eliminate or to account different types of noise (Nistor and Buda, 2016a; Nistor and Buda, 2016b). While the first-order ionospheric delay can be reduced by the use of dual frequency receivers and a combination of ionospheric-free phase carrier, the delay generated by the troposphere has to be estimated. In contrast to ionospheric delay, the influence of the troposphere cannot be eliminated by using dual frequency receivers and the GPS signal is slowing down and its path is getting curved. By using an appropriate mapping function the tropospheric slant delays (STDs) are mapped to the receiver's zenith direction (de Oliveira Jr. et al., 2016). The resulting Zenith Total Delay (ZTD) by processing GNSS data, which is caused by the tropospheric refraction, is divided into two components: 1) the hydrostatic part called Zenith Hydrostatic Delay (ZHD) and 2) the non-hydrostatic delay part called Zenith Wet Delay (ZWD) (Davis et al., 1985) or Wet Tropospheric Delay (WTD). The ZHD can be relatively easily modeled with high accuracy from surface temperature and pressure using the laws of the ideal gases. Nonetheless, the effect of the ZHD varies with local atmospheric pressure and temperature in a really predictable manner and its variation is less than 1 % in a few hours, which can be corrected with an a priori model such as Saastamoinen model (Saastamoinen, 1972). But this is not the case for ZWD, which depends on the amount of water vapor in the atmosphere, which has the property to vary very quickly in time and space (Nistor and Buda, 2015a; Nistor and Buda, 2016c). The ZWD also has to be estimated, because the combination of the observations cannot mitigate the effect of the delay and the only way to reduce the effect of the troposphere, is to use models and/or to estimate it from observational data.

Cite this article as: Nistor S, Buda AS: Evaluation of the ambiguity resolution and data products from different analysis centers on zenith wet delay using PPP method. Acta Geodyn. Geomater., 14, No. 2 (186), 205–220 , 2017**.** DOI: 10.13168/AGG.2017.0004

To obtain the position on centimeter level accuracy, it takes about 30 minutes of measurements, due to the enlarged noise of ionosphere-free combination and the existence of phase ambiguities (Bisnath and Gao, 2009; Nistor and Buda, 2015b). In order to improve the accuracy of the determination and shorten the necessary time for integer ambiguity fixing, different approaches have been developed in recent years (Ge et al., 2008; Collins et al., 2010; Bertiger et al., 2010; Loyer et al., 2012; Li and Zhang, 2012). This approach replaces the ionosphere-free ambiguities by wide-lane (WL) and narrow lane (NL) ambiguities with a wavelength of 86 and 11 cm respectively, in the case of GPS constellation. With the help of pseudorange observations the wide-lane ambiguity is resolved by using the Melbourne–Wübbena (MW) combination. Geng et al. (2011) recommended that it's necessary 10 minutes of observation for determining 90 % of wide-lane ambiguities with enough reliability. In the case of the narrow-lane, this can be resolved only after the wide-lane ambiguities have been fixed and the necessary time for collecting the observations in this case is around 20 minutes, due to the presence of the bias in the estimated uncalibrated phase delays (UPDs) and the short wavelength of the narrow-lane ambiguity. The time dependent UPD correction for narrow lane ambiguities presents a higher reliability than those of daily average, which leads to a higher ambiguity fixing rate (Ge et al., 2008).

MATERIALS AND METHODS

The un-differenced observation equations for GNSS processing can be written as:

$$P^s_{j,k} = \rho^s_k + c\delta t_k - c\delta t^s + T^s_k + \alpha_j I^s_k + O^s_k + d_{k,p_j} - \\ - D^s_{p_j} + d_{k,others} + \varepsilon^s_{k,p_j} \quad (1)$$

$$\phi^s_{j,k} = \rho^s_k + c\delta t_k - c\delta t^s + T^s_k + \alpha_j I^s_k + O^s_k + b_{k,\Phi_j} - \\ - b^s_{\Phi_j} + d^s_{k,others} + \lambda_j N_j + \varepsilon^s_{k,\Phi_j} \quad (2)$$

where: j is the frequency number, s refers to a given satellite, subscript k refers to the receiver, $P^s_{j,k}$ is the pseudorange measurement (m), $\phi^s_{j,k}$ is the carrier-phase measurement (m), ρ^s_k is the geometric range between the satellite and receiver antenna phase center (m). If the coordinates of the reference station is known with high precision, then the distance is known exactly. c is the vacuum speed of light, δt_k and δt^s represents the receiver and satellite clock offset, T^s_k is the troposphere delay, I^s_k is the ionospheric delay which is related to the signal frequency L_1, α_j is the frequency scaling set as:, $\alpha_j = f_1^2 / f_j^2$, O^s_k represents the satellite orbital error (m), d_{k,p_j}, $D^s_{p_j}$ is the receiver and satellite differential code bias (DCB) between pseudoranges. One important aspect is that the bias is related to the frequency. The $d_{k,others}$ represents the other error which influences the measurements such as plate motions, multipath delay, tidal correction, etc. b_{k,Φ_j}, $b^s_{\Phi_j}$ are the receiver and satellite carrier phase fractional bias at L1 and L2 frequency, N_j is the carrier-phase ambiguity (cycles) at frequency j and λ_j is the carrier wavelength. ε^s_{k,p_j} and ε^s_{k,Φ_j} represents the measurement errors of carrier-phase and pseudoranges.

The GPS signal changes the speed and the path as it travels through the atmosphere, in comparison by traveling into the vacuum. The delay caused by the tropospheric refraction can be expressed as (Leick et al., 2015):

$$\delta\rho = \int n(s)\,ds - \int ds \quad (3)$$

where $\delta\rho$ is the tropospheric delay and $n(s)$ represents the refractive index as a function of the path. The zenith tropospheric delay is divided into two components: zenith hydrostatic delay (ZHD) and zenith wet delay (ZWD) or wet tropospheric delay (WTD). The total amount of tropospheric delay is a sum of the two components:

$$ZTD = ZHD + ZWD \quad (4)$$

where ZTD is the zenith total delay, ZHD is the zenith hydrostatic delay and ZWD is the zenith wet delay.

The problem arises when ZTDs are mapped into slant tropospheric delay, by using the mapping functions, which can introduce significant errors in the estimation. By converting or mapping the zenith delays into slant delays, it is recommended to use accurate and proper mapping functions due to the fact that for low elevations angles (<15 degrees) the slant delay can be ten times larger than for the zenith direction (Prasad and Ruggieri, 2005). The slant total delay (STD) is computed by using the following formula:

$$STD(e) = ZHD * m_d(e) + ZWD * m_w(e) \quad (5)$$

where (e) is the elevation angle towards the satellite, $STD(e)$ represents the total slant delay, ZHD is the hydrostatic zenith delay, $m_d(e)$ mapping function used for the hydrostatic delay, ZWD is the zenith wet delay and $m_w(e)$ represents the mapping function for the wet delay. Nowadays the best results are provided by the Vienna Mapping Function (VMF1) which is derived from the numerical weather model and the empirical Global Mapping Function (GMF) (Boehm et al., 2006).

The core products from IGS are assured by nine IGS AC's, which are responsible for assuring final, rapid and/or ultra-rapid data products. The Associate Analysis Centers from IGS (AACs) are responsible for the "non-core" products. The IGS Analysis Center Coordinator (ACCs) retrieves each individual contribution and generates a set of combined products

Table 1 Analysis strategy summary for ESA and JPL.

Analysis Center	ESA	JPL
Software used	NAPEOS	GIPSY/OASIS-II
Basic observables	❖ Undifferenced carrier phases and pseudoranges ❖ Data weight, LC: 1 cm ❖ Data weight, PC: 1 m ❖ Weighting: Sigma^2=1/sin(e)	➢ Undifferenced ionosphere-free carrier phase, LC ➢ Undifferenced ionosphere-free pseudorange, PC ➢ Data weight, LC: 1 cm ➢ Data weight, PC: 1 m ➢ Weighting: Sigma^2=1/sin(e)
Modeled observable	Undifferenced, corrected for 1st order ionosphere effect by forming ionospheric free linear combination	Undifferenced LC and PC combinations CA-P1 biases from CODE applied
Troposphere a priori model	❖ Zenith delay computed using the Saastamoinen model with pressure and temperature from the GPT model. The resulting zenith delay is mapped using the dry GMF mapping function. ❖ gradient model: none	➢ A priori model: Wet and Dry from GPT2 model. ➢ Estimation: Zenith delay and horizontal gradients
Ionosphere	❖ 1st order effect: accounted for by dual-frequency observations in linear combination ❖ 2nd order effect: no corrections applied	➢ 1st order effect: Removed by LC and PC combinations ➢ 2nd order effect: Modeled

that are considered the official product of IGS. Throughout the combination process the results are regarded as more robust then individual AC products. A disadvantage is that no GPS software is fully consistent with the combined IGS products. Each Analysis Center has its own strategy for obtaining the data products, where the IGS data products are a combination of each individual data products provided by the AC's and AAC's. In Table 1 the ESA and JPL analysis strategy is resumed – more information can be found at (http://acc.igs.org/reprocess2.html).

The formal uncertainty of the combined orbit form the different Analysis Centers is given by:

$$\sigma^2 = \frac{\sum_{j=1}^{N} W_j * \left(RMS_j\right)^2}{(N-1)\sum_{j=1}^{N} W_j} \quad (6)$$

where the W_j are the AC weights, N is the number of the ACs used and RMS_j is computed from the AC orbit difference by:

$$\left(RMS_j\right)^2 = \sum_{t=1}^{M} \frac{\left(X_j - \bar{X}\right)_t^2 + \left(Y_j - \bar{Y}\right)_t^2 + \left(Z_j - \bar{Z}\right)_t^2}{3M - 7} \quad (7)$$

with $\left(X_j, Y_j, Z_j\right)$ represents the time series of geocentric satellites coordinates for ACj, $\left(\bar{X}, \bar{Y}, \bar{Z}\right)$ the time series of weighted average of geocentric satellite coordinates and M represents the number of ephemeris epochs from ACj.

PROCESSING AND RESULTS

Data from eight European IGS stations were processed: BUCU, BZRG, GANP, GOPE, GRAZ, PADO, PENC and WROC.

The analyzed data is from January 2015. The processing was done using the PPP technique with the help of the Jet Propulsion Laboratory's software GIPSY/OASIS II (Zumberge et al., 1997). The precise ephemeris and clocks were taken from the following sources: European Space Agency (ESA), International GNSS Service (IGS) and from Jet Propulsion Laboratory (JPL). The general settings for precise point positioning determination were:

- Orbit and clock products: precise fiducial orbit and clock – from ESA, IGS and JPL. These data were the final data products.
- The wide lane phase bias information were from JPL.
- Processing was done in static mode, at 300 s interval.
- Elevation cutoff angle of 15^0.
- Antenna phase center variation and antenna phase center offsets– igs08_1884.
- To eliminate the first order ionospheric delays, the ionospheric free phase (LC) combination and ionospheric free range (PC) were used,
- To model the effect of the second ionospheric correction, the model from International Reference Ionosphere (IRI) was applied.
- Number of iterations for ambiguity resolution: in the first stage was set to zero – no ambiguity resolution and in the second stage was set to 2.
- Tide models taken into account from IERS standards: solid Earth tide, ocean tide model and the polar tide model.
- Mapping function: Vienna Mapping Functions 1 – VMF1.

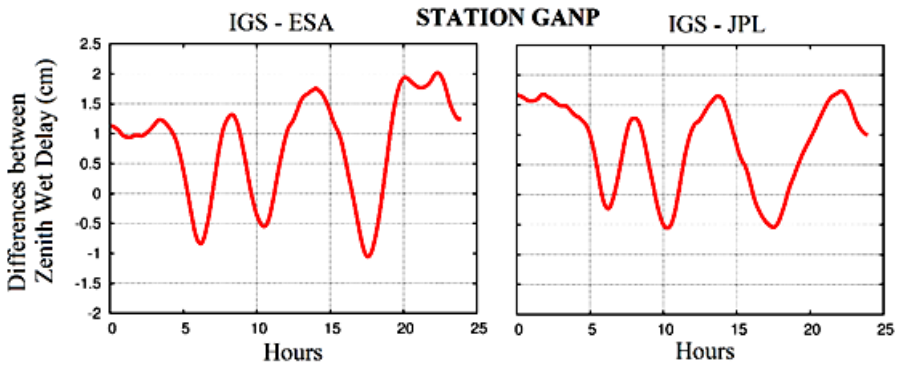

Fig. 1 Differences between Zenith Wet Delay by using precise ephemeris and clock from IGS, ESA and JPL – Station GANP.

- Troposphere estimation parameters: random walk set to 5 cm/sqrt(sec) and wet tropospheric gradient was set to 5 mm/sqrt(sec).
- The weighting scheme was: sqrt(sin(elevation))/sigma.

In the first stage of the study, the impact of precise ephemeris and clock from three Analysis Centers (ACs) were analyzed to monitor their effect on zenith wet delay and on their standard deviation or formal error. By using the data products from IGS, the ionospheric free phase combination (LC) and ionospheric free range combination (PC) presented the lowest values of postfit residuals and thus the best values were generated by them. Because the Zenith Wet Delay presented relatively small difference by using the precise ephemeris and clock from different ACs, we have differentiated between the obtained ZWD when we have used the IGS, ESA and JPL data products. The results are presented in Figure 1.

In Figure 1 the line represents the difference of the Zenith Wet Delay (ZWD) between the estimated values using the precise ephemeris and clock from IGS and ESA – the left part of the plot and IGS minus JPL in the right part of the plot. It can be observed from the plot that the highest difference between the estimated ZWD by using the IGS data products and ESA was on station GANP where they were between -1.2 cm and +2cm during the entire period. The results of the other stations are presented in Appendix A.

In all the cases the solution has been able to converge and the LC postfit residuals presented values from 5 to 10 mm. The highest value namely, 9.75 mm of the LC postfit residuals was calculated on station Graz. For station GANP where the ZWD presented the highest difference, the LC postfit residuals presented a value of 7.4 mm.

The maximum variation on all stations except station GOPE, appeared around the time interval 17.3 - 20 hours. This variation was present around the same time on six out of a total of eight stations. The differences in ZWD by using the IGS and JPL data products, presented a smaller variation. The highest fluctuation was on station WROC with an interval value of -1.4 cm to +1.3 cm around the time interval 17.3 - 20 hours from the beginning of the processing. As in the case of IGS and ESA data products, the station GANP is experiencing a large fluctuation, and the same thing appeared when using the JPL precise ephemeris and clock data – from -0.5 cm to 1.7 cm. In the case of JPL data products, the variation around the same time interval was present on stations BUCU, BZRG, GANP and WROC. This time the station GRAZ and PADO presented large variation at the beginning of processing – between the time interval 4 – 5 hours. When using the IGS and ESA data products none of the stations presented a smooth variation, only in the case where we used the data products from IGS and JPL. This smooth fluctuation was present only on station GOPE excepting the data from the first five hours of processing and on station WROC from 0 - 15 hours of processing.

The differences between ZWD by using the IGS, ESA and JPL data products cannot be attributed to their precision, because the ZWD standard deviation is much smaller than the fluctuation itself. The ZWD's standard deviation (one sigma standard deviation) or formal errors are presented in Figure 2 for station GOPE and the results for the other stations are presented in Appendix B.

In Figure 2 the upper panel represents the standard deviation of the ZWD for station GOPE, computed by using the precise ephemeris and clock from IGS and ESA and the lower panel represents the standard deviation of the ZWD by using the data products from IGS and JPL. The solid line in both panels represents the standard deviation of the ZWD by using the data products from IGS, the dashed line from upper panel represents the standard deviation of the ZWD generated by ESA data products and the dashed line from lower panel represents the standard deviation of the ZWD by invoking the JPL precise ephemeris and clock. When analyzing the upper plot, we can observe that there is no noticeable difference between the resulted standard deviation by using IGS and ESA data products. The estimated standard deviation from IGS and ESA present an overlapping behavior during the entire period, only with very small variations especially in the beginning of the processing at the first hour. The highest variation in terms of ZWD standard deviation was for stations GOPE which presented a mean value of 2.5 mm. Although station GOPE presented the highest mean value of the ZWD standard deviation, the value of the ZWD resulted in a smoother behavior after the first five hours of processing.

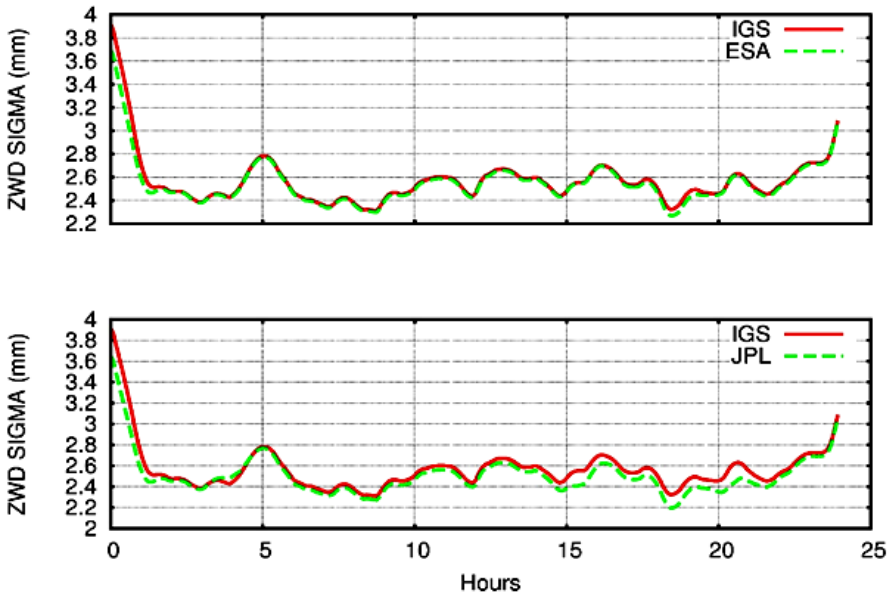

Fig. 2 The standard deviation of the ZWD using the data products from ESA, IGS and JPL – Station GOPE.

Returning to Figure 1 and analyzing the data from Appendix B, where the results by using the IGS and ESA data products are presented in the left part of the plot and IGS and JPL data products in the right part of the plot, we can observe that the variation of approximately 2.7 cm of the ZWD on station WROC from Figure 1, cannot be attributed to the ZWD formal error, because the level of the uncertainty presents a mean value of around 2.3 mm, excluding the first hour of processing. Very small differences appear on stations BUCU, GOPE, GRAZ and PENC which are presented in Appendix B. In these stations, it can be seen that the solid line doesn't overlap perfectly the dashed line.

If we analyze the plot from Appendix B, the right part of the plot, where we have used the data products from IGS and JPL, it can be observed that compared to the left part of the plot, the dashed and solid line don't overlap perfectly on neither of the stations. Regarding the standard deviation generated by JPL compared to the IGS – we can notice a small bias when referring to JPL data products, thus it can be a result of the software developed by an individual AC. Another issue is that the IGS products are not fully consistent with the specific GPS software – in our case GIPSY software.

Compared to the left part of the plot, the right part of the plot presents more noticeable differences, namely the highest difference on the ZWD standard deviation generated by the IGS and JPL data products was about 0.2 mm, which can be seen on station BUCU around 15 hours from the beginning of processing. The highest level of the uncertainty was on all stations in the first hour of processing, which can be attributed to the necessary time for resolving the ambiguity term. Thus the station GOPE presented the highest ZWD standard deviation of 3.87 mm. Also, at the end of the processing time it can be observed an increase of the standard deviation on all stations. Another interesting behavior is observed on station GANP - see Figure 1, where during the entire period there is a significant variation. In Appendix B we can notice that the ZWD standard deviation presents a relatively linear behavior, thus implying that the resulted ZWD is determined quite well. We can conclude that the variation of ZWD that can be seen in Appendix A, is directly linked to the standard deviation of the ZWD that is presented in Appendix B, where approximately during the same time interval, all the stations presented the same fluctuation in terms of ZWD standard deviation.

Another important impact on ZWD determination is represented by the ambiguity resolution. The results are presented in Figure 3 for station GANP and in Appendix C for other stations.

The upper part of this figure presents the results by using the ESA data products, the middle part the results by using the IGS data products and the lower part the results by using JPL data products. The solid line represents the value of the ZWD with resolved ambiguities and the dashed line the ZWD value when no ambiguities were resolved. In the case where no ambiguity was solved, the ZWD behaves more sinuous, but in the case when the ambiguity was resolved the behavior of ZWD presents sudden changes over the course. The station GANP presents the most unusual behavior with sudden changes especially between the time interval 15 and 21 hours when using the IGS data products, we notice that the solved and unresolved ambiguities, in the case when the ZWD is computed, there is a tendency of going opposite directions.

In the case where the ESA data products were used, stations PADO and GANP presented the highest difference – around 6 mm between the solved and unresolved ambiguity – see Appendix C, where the used ESA data products are in the left part of the plot, the IGS data products in its center and its right part

the results by using the JPL data products. Although the ambiguity resolution in the case of PPP needed some time – 30 minutes or more, the ZWD doesn't present high variations at the start of the processing. In the case of stations BZRG, GRAZ and WROC there is a tendency of the same behavior in the first eight hours of processing. They are in agreement at the level of 2-3 mm and no sudden spikes are present (see Appendix C). This type of behavior can be seen on stations BUCU and GOPE, but this time for the first station, is between the time interval 14 to 18 hours and for the second one between the time interval 17 to 21 hours. In the case of station WROC the same behavior remains during the whole 24 hours period. This type of behavior can be seen on stations BZRG, PADO and PENC but on a smaller scale. It can be seen that the ZWD for all stations except the IGS data products, at the end of the processing – especially the last hour of processing, tends to "touch", in both cases: resolved and no ambiguities resolved. The largest difference at the end of processing was 4 mm in the case of stations BUCU and GOPE. The rest of the stations presented a difference of around 1 mm. We can notice that this sudden change appears on the same time period and it is not necessary to relate it to meteorological conditions. Only on station WROC the highest amount of rainfall – around 16 mm/square meter was experienced. The other stations influenced by rainfall were GANP and PENC. On the other stations during the processing period no rainfall was recorded.

In the case of IGS precise ephemeris and clock data, the highest difference of ZWD was recorded on station GANP – around 15 mm, between the solved and unresolved ambiguity. In this case, where IGS data products were used, compared to the ESA data products, stations BZRG, GRAZ and WROC in terms of ZWD present higher differences during the same period, except station WROC in which the trend of the ZWD between the two solutions, perform the same during the whole period. At the same time, the station BZRG presents noticeable spikes and changes of tendency unlike the station GRAZ, where during the whole period there are only small variations. The overlapping behavior of the ZWD at the beginning of processing can be seen on stations GRAZ, PADO and WROC. A large difference in ZWD which was computed by solving and unresolving the ambiguity, at the start of the processing for stations BUCU, GANP, GOPE and PENC resulted a difference of 15 mm. At the end of the processing, the stations GOPE, PENC and WROC present a ZWD that tends to be the same, but the ZWD for the stations BUCU, BZRG, GANP, GRAZ and PADO tends to go in opposite directions. By applying a linear regression for all stations, when the ambiguities were resolved, the determined ZWD presented a higher value than when no ambiguities were resolved. For almost all the stations the solid line is above the dashed line.

When using the JPL data products, the highest ZWD difference was on station PADO – around 4 mm between the solved and unresolved ambiguities. Another station that presented a higher variation is the

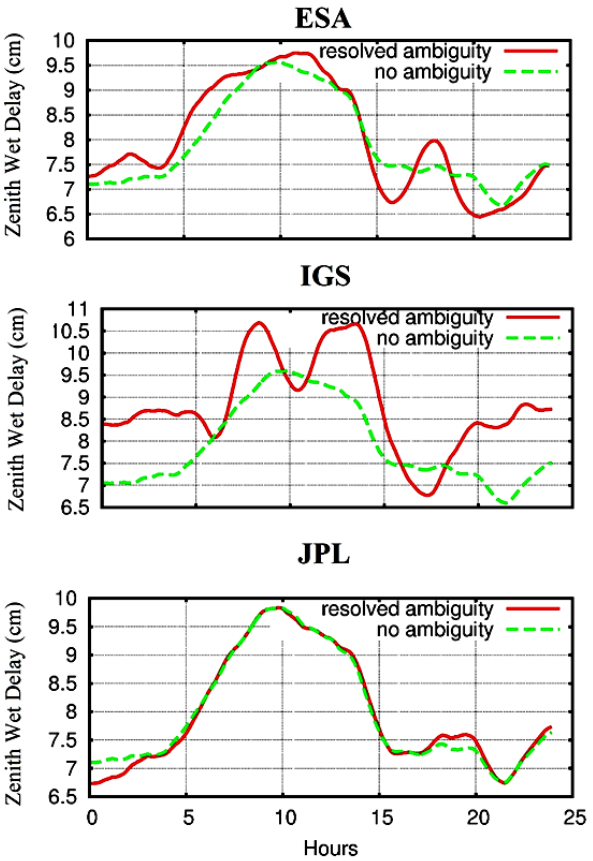

Fig. 3 The impact of the ambiguity resolution on Zenith Wet Delay – Station GANP.

station GANP, but only for a relatively short period – approximately one hour, from 18 till 19 hours. In the case of precise ephemeris and clock data from JPL, the computed ZWD when the ambiguity was resolved, overlaps the computed ZWD when no ambiguity was solved during the entire processing time on all the stations. Station BUCU only at the beginning and at the end of the processing presented a small difference of the computed ZWD between the solved and unsolved ambiguity and for the rest of the processing time the two solutions mentioned before were the same. This type of the behavior was also present on the station GANP and the rest of the stations presented the maximum difference of 2 mm. Also the trend of the ZWD on station GANP is almost the same during the remaining period, presenting variations at the beginning and at the end of the processing.

DISCUSSION

All the stations except station WROC, in the case of IGS data products, the ambiguity resolution generates a "spiky" behavior of ZWD compared to the data where no ambiguity was resolved. In the case of station GANP the ambiguity resolution doesn't create only a "spiky" behavior, but also has a tendency of going opposite directions, especially between the time interval 7 to 13 hours from the beginning of processing. The estimated ZWD where the ambiguity resolution was solved presented the highest variations on all the stations, in the case where the IGS data products were used. This "spiky" behavior and the large variations in the case of using IGS data products

can be attributed to the fact that the IGS data products are a combination of data products from nine different Analysis Centers with different strategies: combining both undifferenced carrier phases and pseudoranges with doubly differenced observation modelling strategy. In the case of the used software the data products from IGS is not fully consistent with the software strategy. It seems that by using the ESA data products, which are obtained by using the undifferenced carrier phase's modelling strategy, the effect of "spiky" behavior and large variations are reduced.

Comparing the ZWD, with and without ambiguity resolution using ESA at the beginning of the processing, the ZWD is much closer for five of the stations: BUCU, BZRG, GANP, GOPE and PENC. In the case of IGS data products the ZWD for the stations GRAZ, PADO and WROC almost overlapped at the beginning then the ZWD resulted by using ESA precise ephemeris and clock.

In the case of JPL data products the difference in ZWD generated by the ambiguity resolution wasn't noticeable in any of the stations. Comparing the trend of the ZWD during the entire processing time with the results by using the IGS and ESA data products it can be seen that, the JPL data products don't create noticeable differences on ZWD when the ambiguity resolution is solved. Also, this is the only case when the ambiguity resolution doesn't create a "spiky" behavior of the ZWD. This type of behavior, especially generated by the IGS data products can be a result of the fact that the satellite clock combination is disregarding the integer-preserving characteristics of the clock products. In the case of the individual AC, the solutions provided by them are integer clocks data. The IGS data products are considered robust solutions compared to the individual AC solution, due to the possibility of undetected outliers in the individual solution. Another aspect is the hardware delays within GPS measurements, which have to be correctly handled for a reliable Precise Point Positioning Ambiguity Resolution (PPP-AR), but also it is necessary to take into account the AC specific modelling, which is critical to ensure the integer nature of the carrier-phase ambiguity. The different standards adopted by each individual ACs for modelling the yaw manoeuvers during orbit noon and orbit midnight which represents a potential factor for influencing the results, which have to be investigated. Also the ambiguities were resolved by using the JPL's wide lane phase bias, which create the effect of consistency between the data products and software. This effect is called the "software bias" which is the tendency of a given software to perform better when using its own products. The problem is that a potential bias of an individual AC can be absorbed into carrier phase ambiguity.

In all the cases the data products from ESA, IGS and JPL, the ambiguity resolutions in all the stations presented a higher value of the ZWD. The "spiky" behavior of the ZWD in the case when the ambiguity was solved, showed itself for the data products from ESA and IGS, but in the case of the JPL precise ephemeris and clock, the behavior tends to be the same in all the stations.

The importance of the data products and ambiguity resolution is reflected also in the coordinate's estimation among other parameters. The differences in Up component for station GANP are presented in Table 2.

The highest difference in Up component was in the case when the ambiguities were solved, between the results generated by using the IGS and JPL data products, resulted a value of -21 mm. In the case of JPL and ESA data products where the strategy of obtaining the precise orbits and clock data is similar, the difference on Up component is the lowest. When the ambiguities weren't solved, the highest difference is observed in the case of JPL and ESA data products, but compared to the results when the ambiguity was solved, the value +5 mm is the lowest. It seems that the constraint generated for solving the ambiguities by using the wide lane phase bias which is a product of JPL, created a variation on Up component.

In Table 3 the difference on Up component for station GANP between the solved ambiguities and no ambiguities are summarized for the ESA, IGS and JPL data products.

From the results it can be seen that the strategy of obtaining the data products together with using the software developed by the same Analysis Center, can lead to more consistent results.

CONCLUSION

The effect on ZWD generated by the use of data products from different Analysis Centers and ambiguity resolution was assessed through a comparative analysis between different IGS stations. It can be seen, that precise ephemeris and clock information from different AC's influence the determination of ZWD for the same GPS station. The influence of data products from ESA, IGS and JPL was studied in the first part of this paper in which the ambiguities were resolved. The maximum difference of the ZWD was 3 cm, when the IGS and ESA data products were used and appeared in station GANP. The other stations presented a difference in ZWD around 2 cm when using ESA, IGS and JPL data products. This difference appeared around 15 hours from the beginning of the processing. Another influence on ZWD determination is created by the ambiguity resolution. In this case, the station GANP presented the highest difference, but also the high variation on ZWD during the whole processing period. The integer ambiguity resolution (AR) in PPP is more complicated and complex problem compared to double difference processing. It is much more sensitive regarding the quality of used products and their correct interpretation. Therefore, AR in the PPP has to be done very carefully; otherwise ambiguity fixed solution can be worse than float solution in some cases. In light of the presented results it is recommended that not only the ambiguity resolution can be considered an important factor of determining the ZWD but also the precise ephemeris and clock data products have to be taken carefully into attention.

Table 2 Differences in Up component for station GANP by using data products from IGS, ESA and JPL.

	Differences in UP component (mm)		
	IGS-ESA	IGS-JPL	JPL-ESA
With ambiguities solved	-16	-21	+5
No ambiguities	0	+2	-3

Table 3 Differences in Up component for station GANP between the solved ambiguities and no ambiguities.

Data products	ESA	IGS	JPL
Differences (mm)	-7	-23	0

We should also take into account the strategy used for obtaining the data products: undifferenced carrier phases, doubly differenced modelling or a combination of undifferenced carrier phases plus doubly differenced strategy.

ACKNOWLEDGMENTS

We gratefully acknowledge the two anonymous reviewers and the editor for thoughtful comments and suggestions which contributed significantly to improve the quality of the manuscript.

REFERENCES

Bertiger, W., Desai, S., Haines, B., Harvey, N., Moore, A., Owen, S., and Weiss, J.: 2010, Single receiver phase ambiguity resolution with GPS data. Journal of Geodesy, 84 (5), 327–337. DOI: 10.1007/s00190-010-0371-9

Bisnath, S. and Gao, Y.: 2009, Current state of precise point positioning and future prospects and limitations. In: Observing our changing Earth. Springer, 615–623. DOI: 1007/978-3-540-85426-5_71

Boehm, J., Werl, B. and Schuh, H.: 2006, Troposphere mapping functions for GPS and very long baseline interferometry from European Centre for Medium-Range Weather Forecasts operational analysis data. Journal of Geophysical Research, 111 (B2), B02406. DOI: 10.1029/2005JB003629

Collins, P., Bisnath, S., Lahaye, F. and Héroux, P.: 2010, Undifferenced GPS ambiguity resolution using the decoupled clock model and ambiguity datum fixing. Navigation, 57 (2), 123–135. DOI: 10.1002/j.2161-4296.2010.tb01772.x

Davis, J.L., Herring, T.A., Shapiro, I.I., Rogers, A.E.E. and Elgered, G.: 1985, Geodesy by radio interferometry: Effects of atmospheric modeling errors on estimates of baseline length. Radio Science, 20 (6), 1593–1607. DOI: 10.1029/RS020i006p01593

Dixon, K.: 2006, StarFire: A global SBAS for sub-decimeter Precise Point Positioning. In: Proceedings of ION GNSS, 26–29.

Dow, J.M., Neilan, R.E. and Rizos, C.: 2009, The international GNSS service in a changing landscape of global navigation satellite systems. Journal of Geodesy, 83 (3-4), 191–198. DOI: 10.1007/s00190-008-0300-3

Ge, M., Gendt, G., Rothacher, M., Shi, C. and Liu, J.: 2008. Resolution of GPS carrier-phase ambiguities in Precise Point Positioning (PPP) with daily observations. Journal of Geodesy, 82 (7), 389–399. DOI: 10.1007/s00190-007-0187-4f

Geng, J., Teferle, F.N., Meng, X. and Dodson, A.H.: 2011, Towards PPP-RTK: Ambiguity resolution in real-time Precise Point Positioning. Advances in Space Research, 47 (10), 1664–1673. DOI: 10.1016/j.asr.2010.03.030

Heroux, P., Kouba, J., Collins, P. and Lahaye, F.: 2001. GPS Carrier-phase point positioning with precise orbit products. In: Proceedings of the KIS, 5–8.

Leick, A., Rapoport, L. and Tatarnikov, D.: 2015, GPS Satellite Surveying, Fourth Edition. John Wiley & Sons.

Li, X. and Zhang, X.: 2012, Improving the estimation of uncalibrated fractional phase offsets for PPP ambiguity resolution. Journal of Navigation, 65 (03), 513–529. DOI: 10.1017/S0373463312000112

Loyer, S., Perosanz, F., Mercier, F., Capdeville, H. and Marty, J.-C.: 2012, Zero-difference GPS ambiguity resolution at CNES–CLS IGS Analysis Center. Journal of Geodesy, 86 (11), 991–1003. DOI: 10.1007/s00190-012-0559-2

Nistor, S. and Buda, A.S.: 2015a, Using different mapping function in GPS processing for remote sensing the atmosphere. Journal of Applied Engineering Science, 5 (2) , 73-80. DOI: 10.1515/jaes-2015-0024

Nistor, S. and Buda, A.S.: 2015b, Ambiguity resolution in Precise Point Positioning technique: A case study. Journal of Applied Engineering Sciences, 5 (1) , 53-60. DOI: 10.1515/jaes-2015-0007

Nistor, S. and Buda, A.S.: 2016a, GPS network noise analysis: a case study of data collected over an 18-month period. Journal of Spatial Science, 61(2), 1–14. DOI: 10.1080/14498596.2016.1138900

Nistor, S and Buda, A.S.: 2016b, The influence of different types of noise on the velocity uncertainties in GPS time series analysis. Acta Geodyn. Geomater., 13, No. 4 (184), 387–394. DOI: 10.13168/AGG.2016.0021

Nistor, S. and Buda, A.S.: 2016c. The influence of Zenith Tropospheric Delay on PPP-RTK. Journal of Applied Engineering Sciences, 6 (1), 71–76. DOI: 10.1515/jaes-2016-0010

de Oliveira Jr., P.S., Morel, L., Fund, F., Legros, R., Monico, J.F.G., Durand, S. and Durand, F.: 2016. Modeling tropospheric wet delays with dense and sparse network configurations for PPP-RTK. GPS Solutions, 1–14, DOI: 10.1007/s10291-016-0518-0

Prasad, R. and Ruggieri, M.: 2005, *A*pplied satellite navigation-using GPS, GALILEO and augmentation systems.ARTECH HOUSE, 309 pp.

Saastamoinen, J.: 1972, Atmospheric correction for troposphere and stratosphere in radio ranging of satellites. In: Henriksen, S., Mancini, A. and Chovitz, B. (eds), The use of artificial satellites for geodesy. Geophysical Monograph Series, AGU, Washington DC, 15, 247–251.

Zumberge, J.F., Heflin, M.B., Jefferson, D.C., Watkins, M.M. and Webb, F.H.: 1997, Precise Point Positioning for the efficient and robust analysis of GPS data from large networks. Journal of Geophysical Research, 102 (B3), 5005. DOI: 10.1029/96JB03860

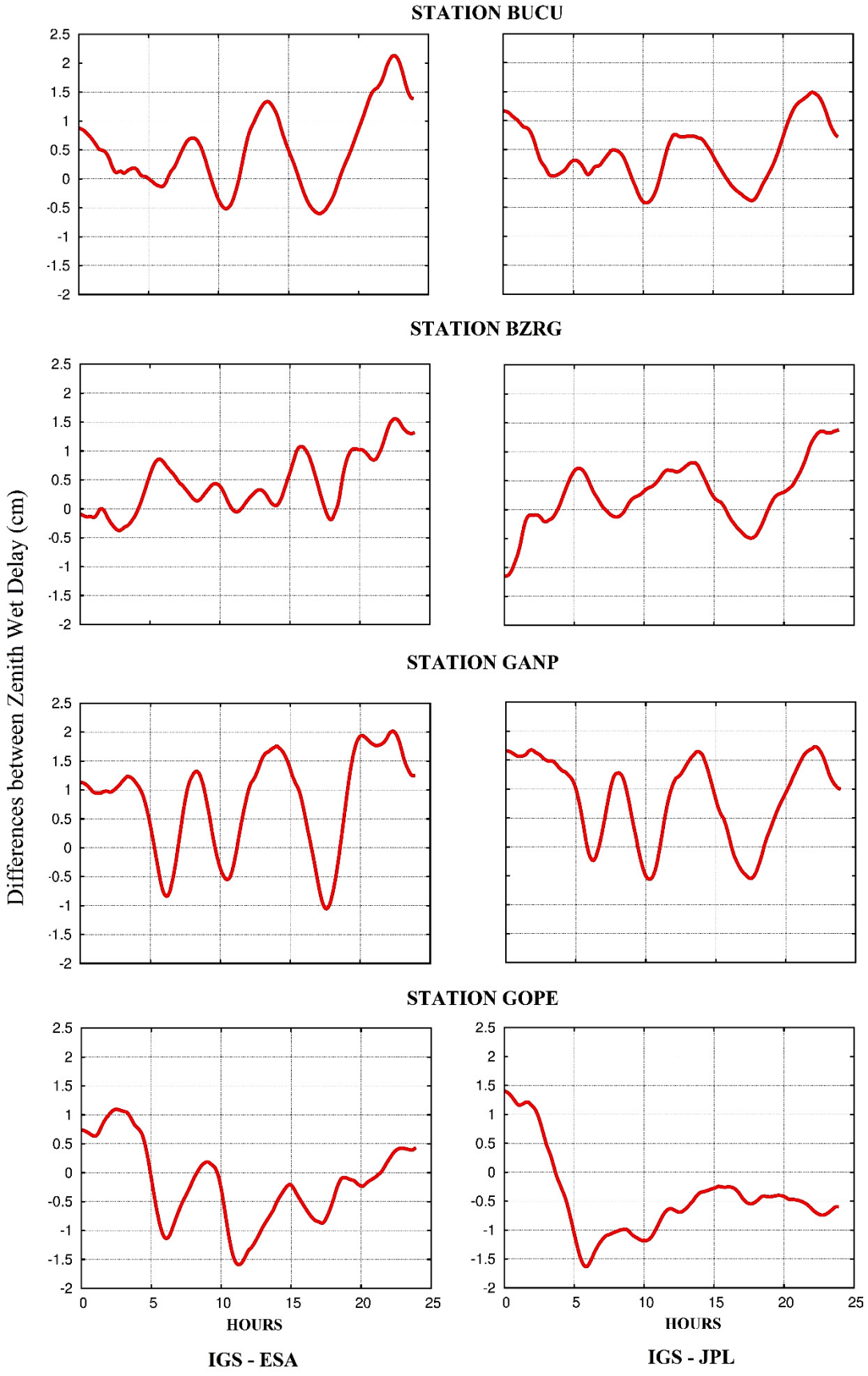

Appendix A: Differences between Zenith Wet Delay by using precise ephemeris and clock from IGS, ESA and JPL – Figure 1.

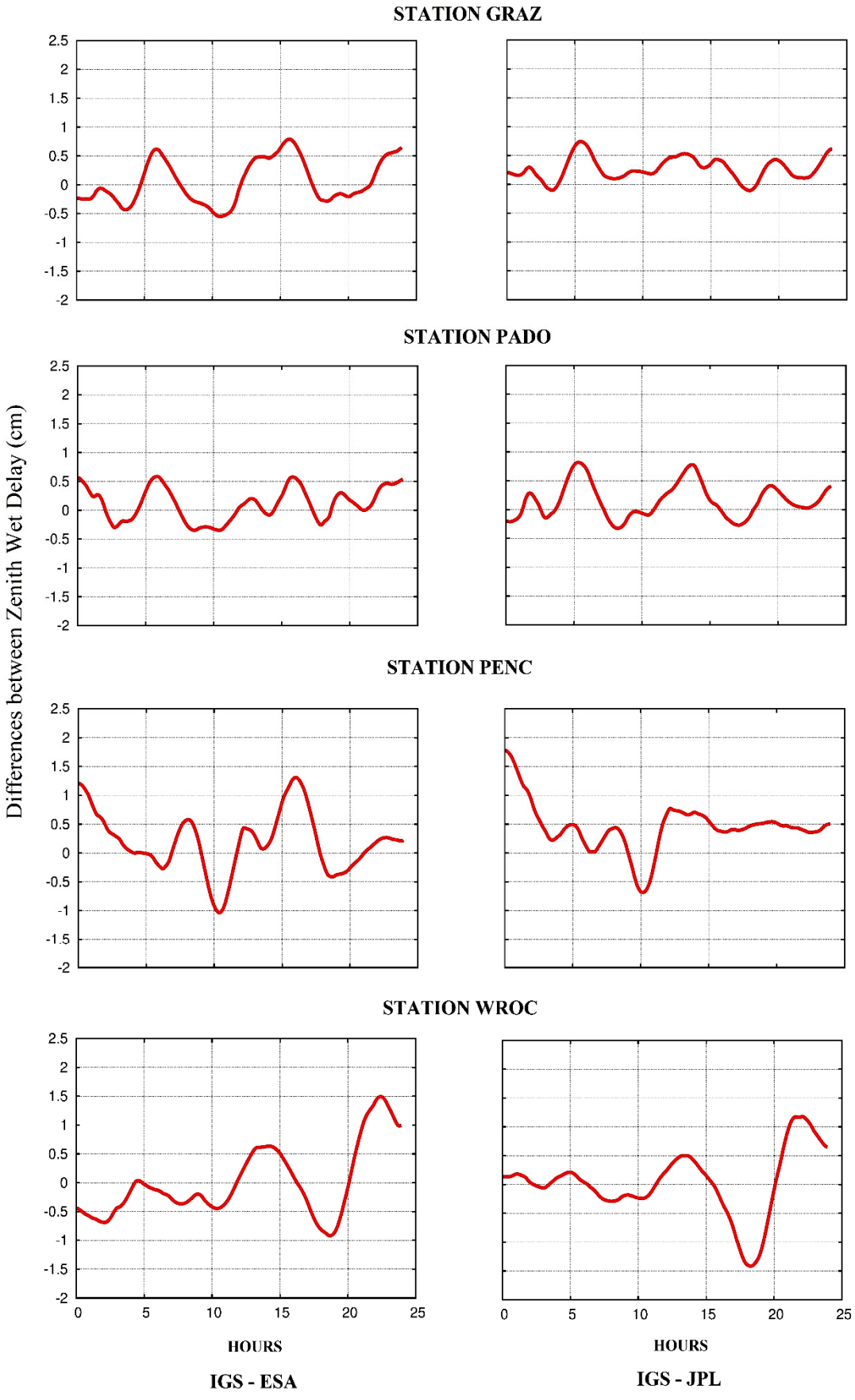

Appendix A: Figure 1 (Continued).

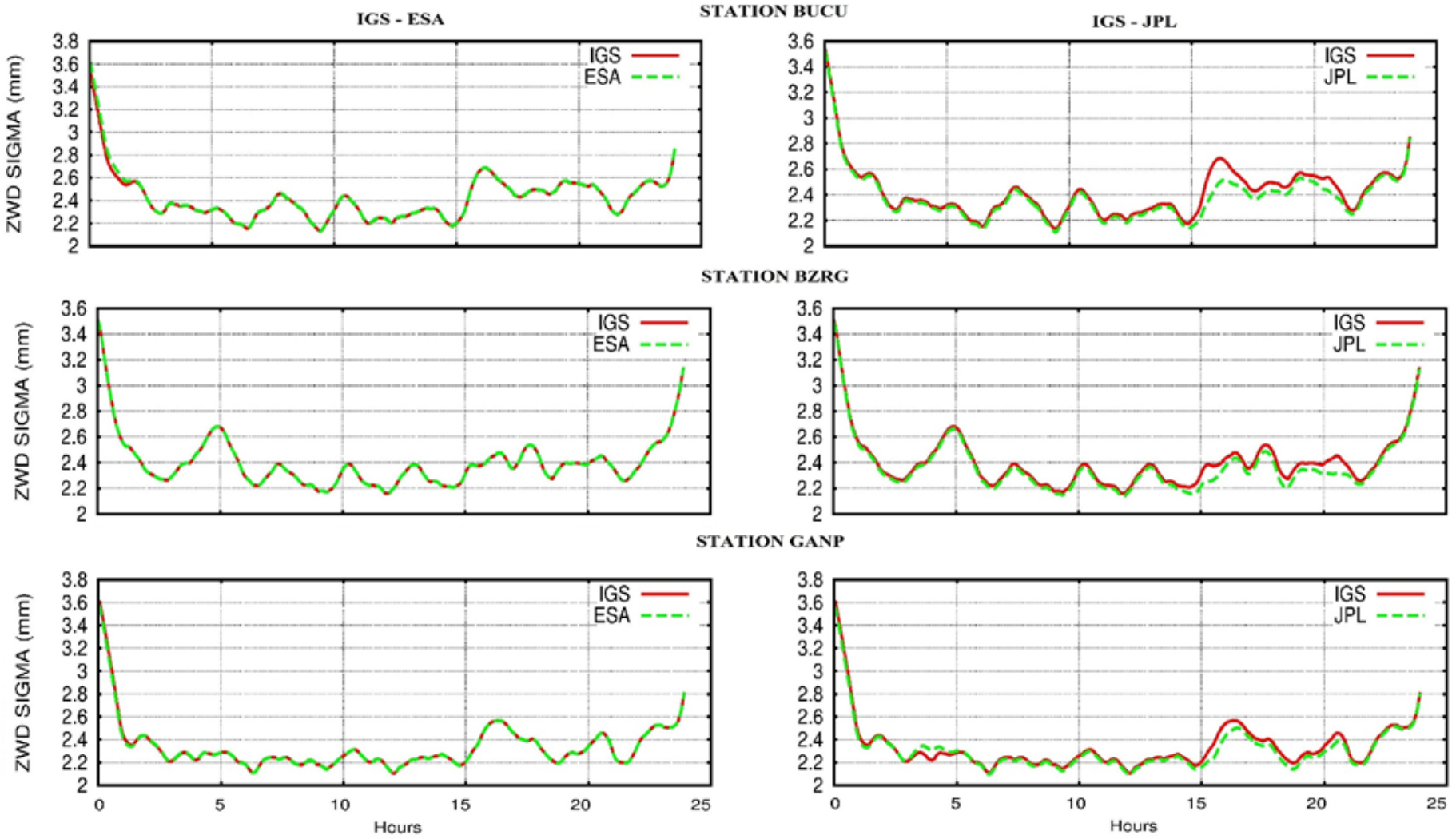

Appendix B: The ZWD standard deviation using the data products from ESA, IGS and JPL – the left part is IGS-ESA and the right part is IGS-JPL – Figure 2.

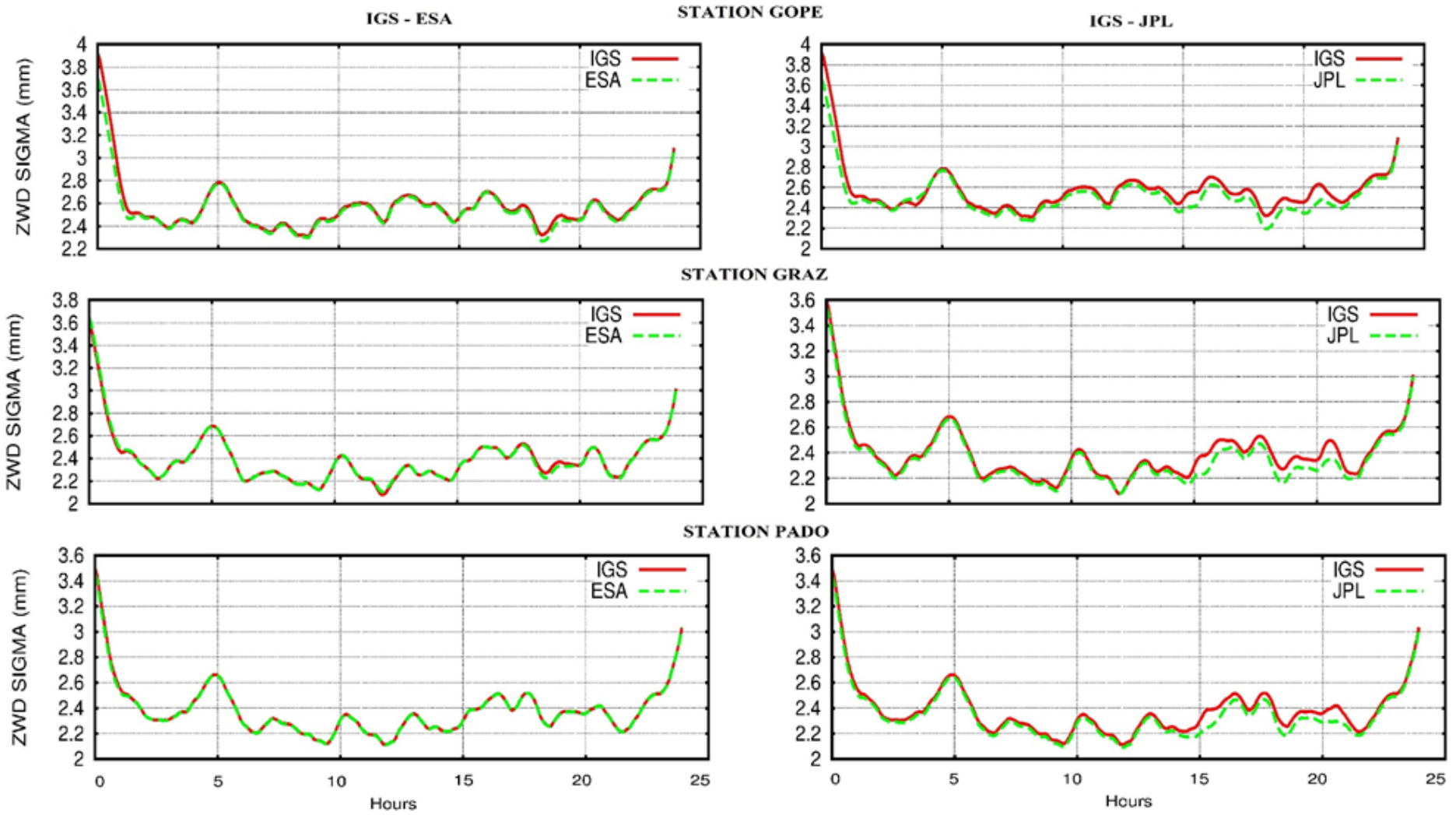

Appendix B: Figure 2 (Continued).

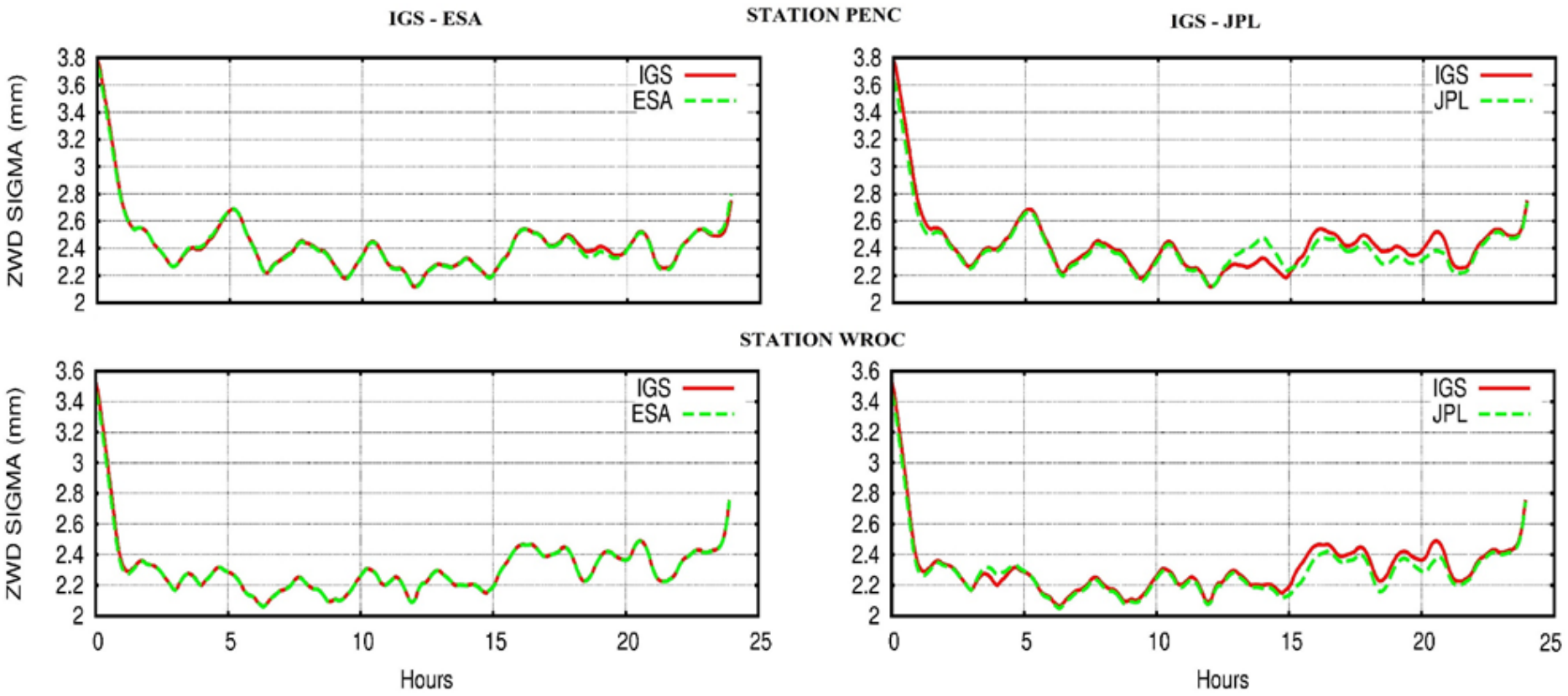

Appendix B: Figure 2 (Continued).

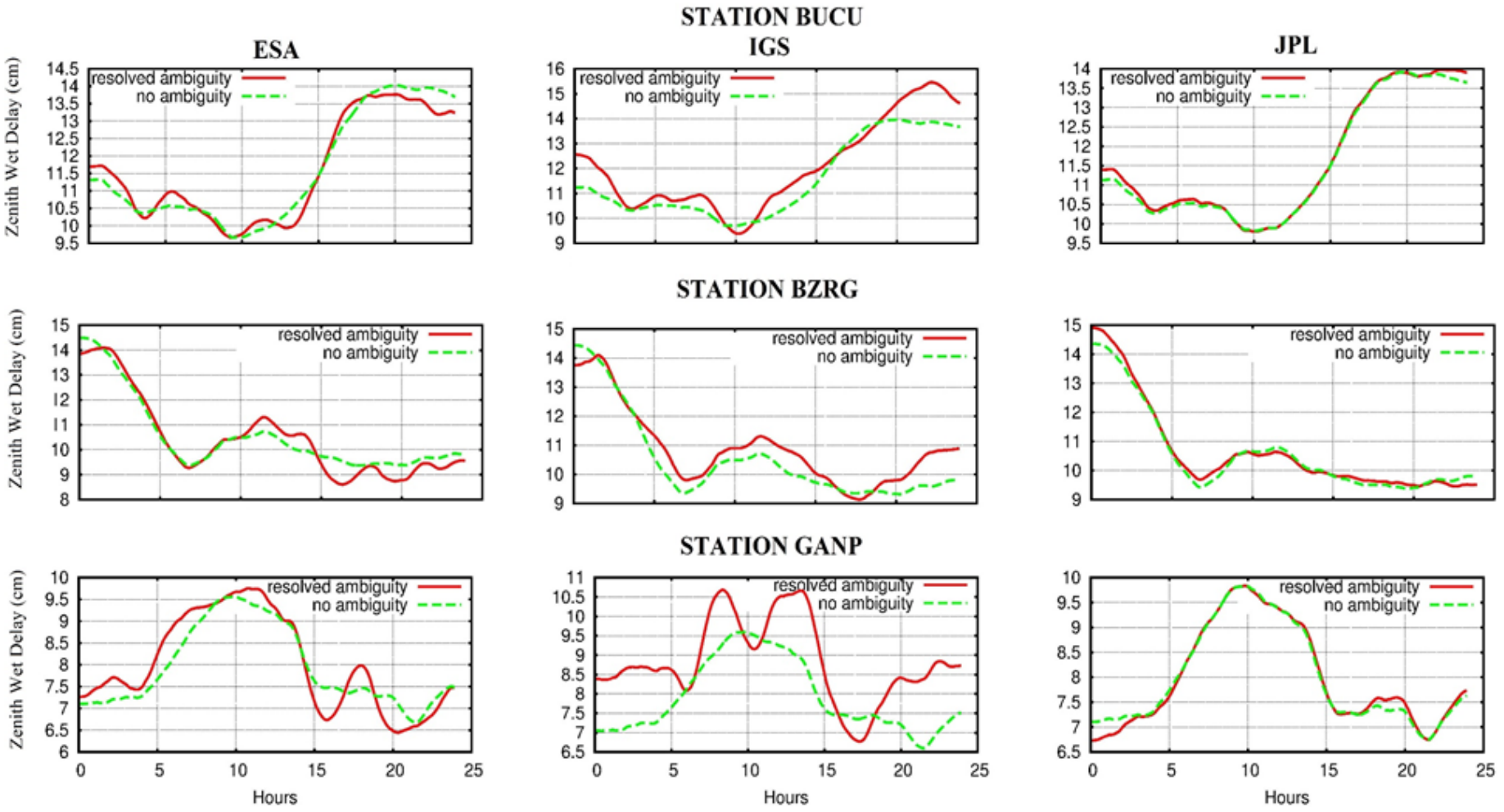

Appendix C: Impact of the ambiguity resolution on Zenith Wet Delay using –left ESA, middle IGS and right JPL data products – Figure 3.

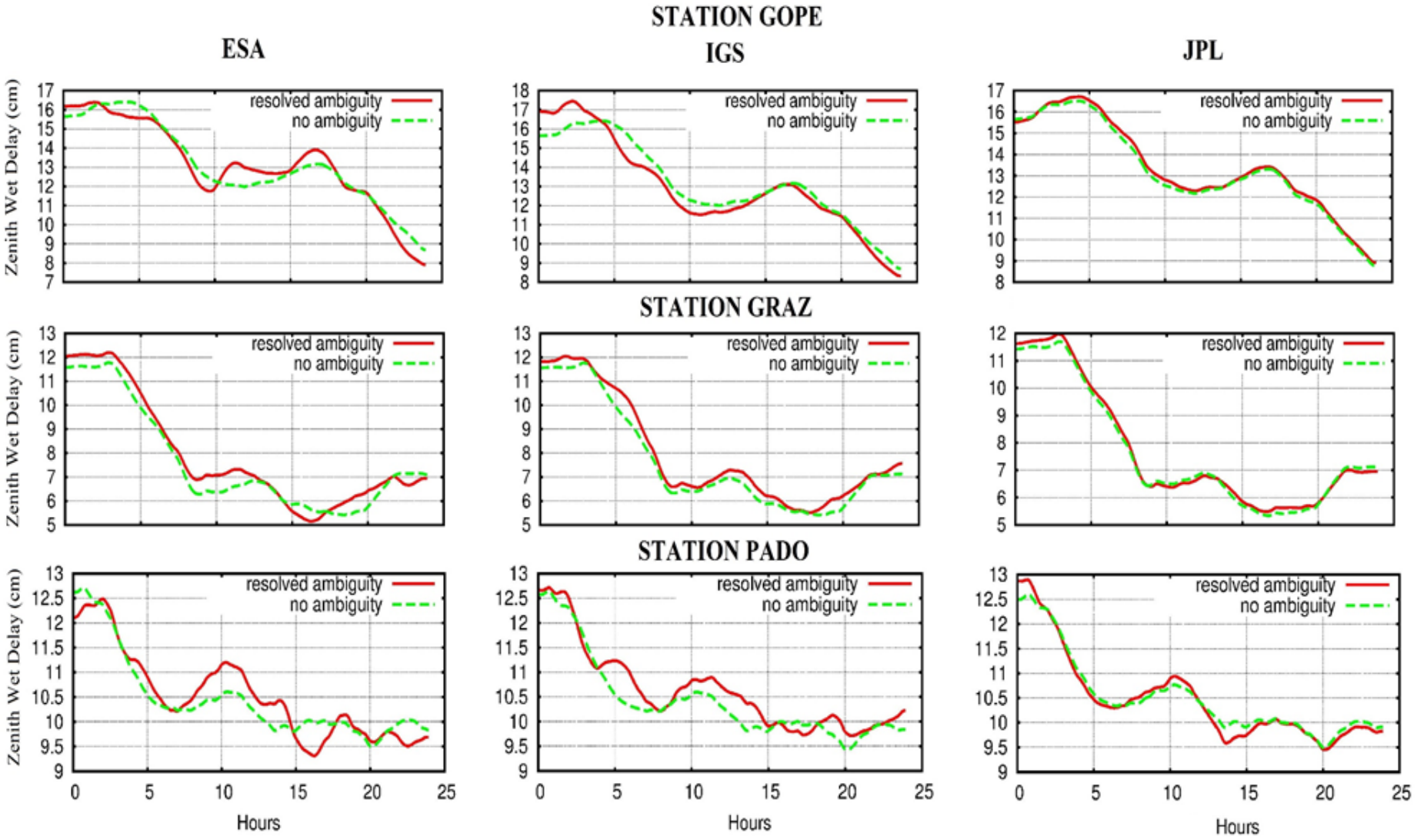

Appendix C: Figure 3 (Continued).

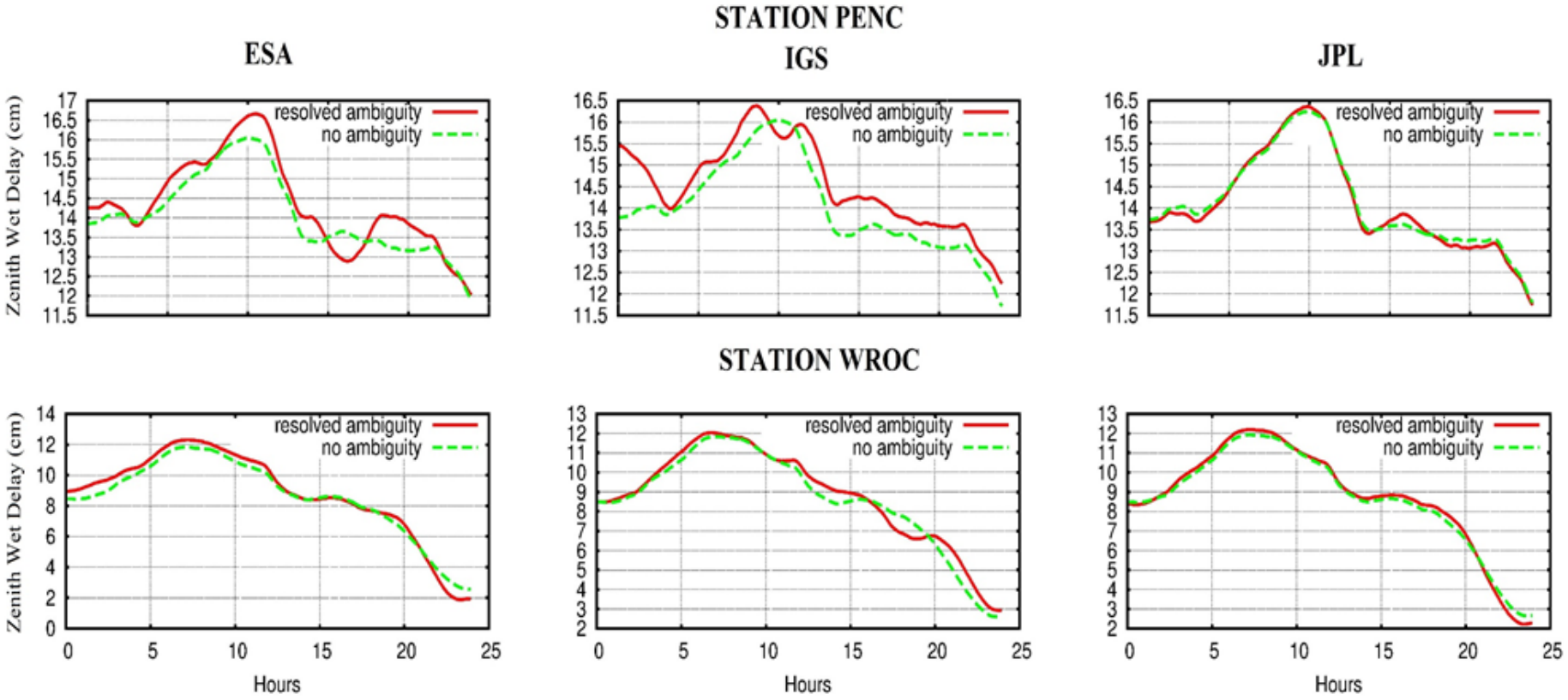

Appendix C: Figure 3 (Continued).